Steady-state isothermal bounded plasma with neutral dynamics

J.-L. Raimbault, L. Liard, J.-M. Rax, and P. Chabert
Laboratoire de Physique et Technologie des Plasmas, Ecole Polytechnique, 91128 Palaiseau, France

A. Fruchtman and G. Makrinich
Sciences Department, Holon Institute of Technology, 52 Golomb Street, Holon 58102, Israel

(Received 10 October 2006; accepted 28 November 2006; published online 16 January 2007)

The Tonks-Langmuir, Godyak, and Schottky steady-state isothermal models are extended when the dynamics of the neutral gas is taken into account. Exact analytic quadratures for the electron temperature, densities, and potential profiles are obtained for these three models within the plasma approximation. It is shown that, contrary to the uniform neutral pressure case, the particle and the power balance are both necessary to determine the electron temperature when neutral dynamics is included. When neutral dynamics is governed by collisions with ions, the neutral density that results from ionization is predicted to have a minimum at the center of the discharge, as indeed is observed in experiment. It is found that even a small amount of ionization can result in a rather strong neutral depletion. However, when the drag on neutrals due to collisions with ions is negligible, the predicted profile of the neutral density that results from intense ionization is reversed and exhibits an unexpected maximum at the center of the discharge. © *2007 American Institute of Physics*.
[DOI: 10.1063/1.2424558]

I. INTRODUCTION

There are three well-established steady-state transport theories covering the full range of neutral pressures used in conventional plasma discharges. These three regimes can be classified by comparing the ion mean free path λ, with the characteristic length L of the discharge. Since $\lambda=(n_n\sigma)^{-1}$, where n_n is the neutral density (proportional to the neutral pressure p) and σ is the total ion-neutral cross section, a relevant quantity, known as the similarity parameter, is the product of the pressure with the discharge length; i.e., pL. At very low pressures ($pL<0.1$ mTorr m), the standard approach is the kinetic theory developed by Tonks and Langmuir, as given in Ref. 1. In the opposite limit of high pressure ($pL>10$ mTorr m), the relevant work is the ambipolar fluid diffusion theory of Schottky, presented in Ref. 2. These two seminal papers, written in the early days of plasma discharge studies, predict quite different density and potential profiles, each of which is in reasonable agreement with experimental measurements in the appropriate pressure range. More recently, Godyak has proposed a modified fluid model that bridges the gap between the low- and high-pressure regimes in Ref. 3. All these works assume that the plasma is quasineutral (Poisson equation is discarded and thus the sheath formation is not taken into account), that the electron and ion temperatures are uniform in all the discharge column, and that the ionization rate is so small that the neutral pressure is uniform and unaffected by the plasma formation.

In a recent work, Fruchtman *et al.*, as given in Ref. 4, have studied the dynamics of plasma and neutral gas in pressure balance within the isothermal and quasineutral approximations. These authors formulated and solved an extension of the Schottky model, whereas the Godyak case was only formulated. In the present paper, the solution of the Schottky model is described in detail together with numerical examples, and we show that the Godyak model can be solved exactly by quadratures. In addition, we investigate the low-pressure regime and solve exactly a generalization of the conventional kinetic Tonks-Langmuir model with neutral dynamics. We give explicit relations for the electron temperature for these three models. Contrary to the uniform neutral pressure case, the electron temperature is not only determined by the similarity parameter pL, but also by the plasma density at the center of the discharge; i.e., n_0. Since n_0 is fixed by the rf power deposited in the discharge, the particle *and* the power balance are both necessary to determine the electron temperature when neutral dynamics is included. As observed in experiment (see, for example, Ref. 5), when the neutral dynamics is governed by collisions with ions (Schottky and Godyak models), the neutral density presents a minimum at the center of the discharge. In the collisionless limit (Tonks-Langmuir model), we find that the profile of the neutral density exhibits an unexpected maximum at the center of the discharge. The paper is organized as follows. The Schottky, Godyak, and Tonks-Langmuir models with neutral dynamics are treated in turn in Secs. II–IV. The results are compared and discussed in the last section.

II. THE SCHOTTKY MODEL WITH NEUTRAL DYNAMICS

We consider the generalization of the Schottky model relevant for high pressures when neutral depletion is taken into account. This model was formulated and solved in Ref. 4. In this section, we give a detailed solution of this model, together with new explicit formulas for the various density profiles and some numerical examples.

The plasma is assumed to contain neutral atoms, singly charged positive ions and electrons, and is limited by insulating walls. Infinite plane geometry with symmetry about the midplane will be considered together with steady-state

conditions. In a plane perpendicular to the plasma column, all physical variables are functions of the single coordinate x. The walls are at $x=\pm L$.

Ions and electrons are created within the plasma at a rate $g(x)\equiv\beta_i n_n(x)n_e(x)$ per unit volume, which is proportional to both the electron density $n_e(x)$ and neutral density $n_n(x)$ (when the neutral density is uniform, $\beta_i n_n$ is the usual ionization frequency ν_i). The charge carriers generated within the plasma flow toward the wall, recombine there, and then reenter the plasma as neutral atoms.

The rate of change of the ion flux $n_i(x)v_i(x)$ is given by

$$\frac{d(n_i v_i)}{dx} = +g(x), \tag{1}$$

where $n_i(x)$ and $v_i(x)$ are the density and velocity of ions, respectively.

The electrons are assumed to be in thermal equilibrium with a uniform temperature T_e. The electron density $n_e(x)$ is then given by the Boltzmann distribution

$$n_e(x) = n_0 e^{e\varphi(x)/k_B T_e}, \tag{2}$$

where k_B is the Boltzmann constant, $\varphi(x)$ the electrostatic potential, and n_0 the electron density at the center of the discharge (this density is fixed by the rf power deposited to the plasma).

The ion momentum conservation is determined by three forces; namely, pressure, electric field, and friction:

$$k_B T_i \frac{dn_i}{dx} = -en_i(x)\frac{d\varphi}{dx} - \nu_c(x)n_i(x)Mv_i(x). \tag{3}$$

In this expression, M and $e=1.6\times10^{-19}$ C are the mass and charge of the ions, respectively, and T_i the uniform temperature of ions. Note that the collision frequency for momentum transfer, i.e., $\nu_c(x)\equiv\beta_c n_n(x)$, is a function of the position x via its dependence on the neutral density $n_n(x)$. Note in addition that we have neglected the velocity of neutrals compared to the velocity of ions in the friction force.

Let us now turn to the basic equations for neutrals. The equation of continuity for the neutral flux is

$$\frac{d(n_n v_n)}{dx} = -g(x), \tag{4}$$

where $v_n(x)$ is the velocity of the neutral fluid. The neutral motion is determined by the same contributions as the ion motion apart from the electric force:

$$k_B T_n \frac{dn_n}{dx} = +\nu_c(x)n_i(x)Mv_i(x), \tag{5}$$

where we have assumed that the neutral temperature T_n is uniform, and that ions and neutrals have the same mass M. Note that there is no internal friction for neutrals since the problem is strictly one dimensional.

Since the sheaths are not taken into account in this model, space charge fields are small, and we assume charge neutrality within the plasma (the so-called plasma approximation):

$$n_e(x) = n_i(x). \tag{6}$$

Equations (1)–(6) define a close set of equations for the five variables: the densities of neutrals $n_n(x)$, the densities of charged particles $n(x)\equiv n_e(x)=n_i(x)$, the ion velocity $v_i(x)$, the neutral velocity $v_n(x)$, and the electrostatic potential $\varphi(x)$.

We solve this problem with the following boundary conditions:

$$v_i(0) = v_n(0) = 0, \quad n_n(L) = n_{nw}, \quad n(L) = 0, \quad \varphi(0) = 0.$$

The conditions on velocities are chosen for symmetry reasons, and we set the origin of the potential at $x=0$. One assumes a fixed neutral density n_{nw} at the wall, a condition which could be relevant if the discharge is connected to large buffers of neutral gases (the case where the total number of neutrals is specified constant, which corresponds to a closed reactor, was treated in Ref. 4 and is also briefly discussed in the last section).

Due to the plasma approximation used in this work, the sheath is not described, and the last boundary condition $n(L)=0$ is only approximate. An alternate approximate choice consists in fixing the velocity at the boundary to the Bohm velocity. It is known (see, for example, Ref. 3) that the density or potential profiles are not very sensitive to these different conditions.

To increase physical insight, it is convenient to introduce dimensionless equations. We choose to normalize the velocities to the Bohm velocity, i.e., $u_B\equiv[k_B(T_e+T_i)/M]^{1/2}$, the electrostatic potential to $-k_B T_e/e$, the densities to the neutral density at the wall n_{nw}, and the distances to the ionization length $\lambda_i\equiv u_B/(\beta_i n_{nw})$:

$$N_n \equiv \frac{n_n}{n_{nw}}, \quad N \equiv \frac{n_e}{n_{nw}} = \frac{n_i}{n_{nw}}, \quad V_n \equiv \frac{v_n}{u_B}, \quad V \equiv \frac{v_i}{u_B},$$

$$\phi = -\frac{e\varphi}{k_B T_e}, \quad X \equiv \frac{x}{\lambda_i}.$$

The set of equations (1)–(6) can then be recast in the following dimensionless form:

$$(NV)' = +N_n N, \tag{7}$$

$$(N_n V_n)' = -N_n N, \tag{8}$$

$$N' = -\tau N_n N V, \tag{9}$$

$$\gamma^{-1}N_n' = +\tau N_n N V, \tag{10}$$

$$\phi = -\ln(N/N_0), \tag{11}$$

where the primes denote the first derivative with respect to the variable X, $N_0=N(0)$, $\gamma\equiv(T_e+T_i)/T_n$, and $\tau\equiv\beta_c/\beta_i$. The two parameters β_i and β_c are related, respectively, to the probability of ionization and of momentum transfer, and hence depend on the gas considered and on the electron and ion temperatures. For argon, $\beta_c=\sigma_i v_{th,i}$, with $\sigma_i\approx10^{-14}$ cm^2 the total cross section for ion-neutral collisions and $v_{th,i}\equiv(8k_B T_i/\pi M)^{1/2}$ the mean ion thermal velocity. A good fit for β_i is given in Ref. 6: $\beta_i=2.34\times10^{-14}T_e^{0.59}\exp(-17.44/T_e)$ with T_e in volts.

For a fixed ion temperature T_i and a given gas, the set of equations (7)–(11) depend on only on the electron temperature T_e and on the density at the center N_0. The relevant boundary conditions are

$$V(0) = V_n(0) = 0, \quad N_n(L/\lambda_i) = 1,$$
$$N(L/\lambda_i) = 0, \quad \phi(0) = 0. \tag{12}$$

The neutral density N_n can be eliminated from Eqs. (7) and (9) with the result

$$(N/N_0)^2 + (\Gamma/\Gamma_w)^2 = 1, \tag{13}$$

with $\Gamma \equiv NV$ and $\Gamma_w \equiv \Gamma(L/\lambda_i)$. Here, we used the boundary conditions $N(L/\lambda_i)=0$, $\Gamma(0)=0$ and the relation $N_0^2 = \tau\Gamma_w^2$. The pressure balance equation obtained from the sum of Eqs. (9) and (10) gives a relation between N_n and N:

$$N_n = 1 - \gamma N, \tag{14}$$

where we used $N_n(L/\lambda_i)=1$. From Eq. (14), we get the neutral density at the center of the discharge, i.e., $N_{n0}=1-\gamma N_0 \leqslant 1$. Hence, we see from this relation, that the neutral depletion effect observed at the center of the discharge is a consequence of the pressure balance between charged particles and neutrals. Taking into account the particular form of Eq. (13), we can expect solutions in the form

$$N(X) = N_0 \cos[f(X)] \quad \text{and } \Gamma(X) = \Gamma_w \sin[f(X)], \tag{15}$$

where $f(X)$ is some function to be found. Using these guesses in (7) together with (14), it is easily shown that f must satisfy the differential equation

$$f'(X) = \tau^{1/2}\{1 - \gamma N_0 \cos[f(X)]\},$$

where we used $\Gamma_w^2 = \tau^{-1}N_0^2$. This equation can be solved with the boundary condition $f(0)=0$:

$$\tan\frac{f(X)}{2} = \frac{1-\gamma N_0}{\sqrt{1-(\gamma N_0)^2}} \tan\left(\sqrt{1-(\gamma N_0)^2}\frac{\tau^{1/2}X}{2}\right). \tag{16}$$

The boundary condition $N(L/\lambda_i)=0$ is equivalent to $f(L/\lambda_i)=\pi/2$, and hence

$$n_{\mathrm{nw}}L = \frac{2u_{\mathrm{B}}}{(\beta_i\beta_c)^{1/2}} \frac{1}{\sqrt{1-(\gamma N_0)^2}} \tan^{-1}\left[\frac{\sqrt{1-(\gamma N_0)^2}}{1-\gamma N_0}\right]. \tag{17}$$

Since u_{B} and γ are functions of T_e, (17) is an equation for the electron temperature T_e. Contrary to the undepleted case, the similarity variable $n_{\mathrm{nw}}L$ is related to the electron temperature T_e *and* to the electron density at the discharge center n_0. Consequently, when neutral dynamics are taken into account, power and particle balance are both necessary to determine the electron temperature.

From (14), it is clear that the case of uniform neutral density corresponds to the limit $\gamma N_0 \to 0$. Taking this limit in (17), we obtain the classical Schottky result:

$$n_{\mathrm{nw}}L = \frac{\pi u_{\mathrm{B}}}{2(\beta_i\beta_c)^{1/2}}. \tag{18}$$

Finally, the full solution in this high-pressure limit can be obtained after some algebra in closed form, from Eqs. (14)–(17):

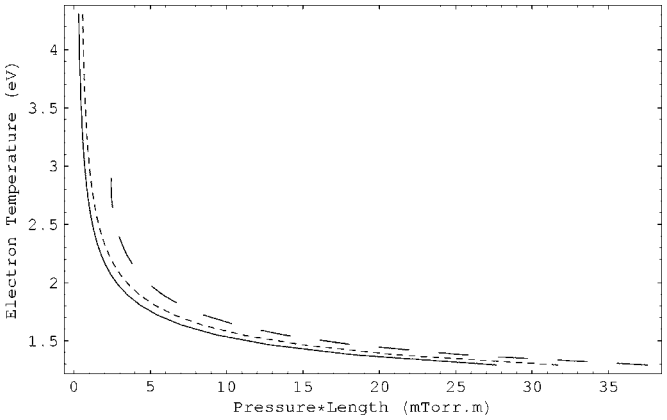

FIG. 1. Electron temperature T_e (in K) as a function of the similarity parameter pL (in mTorr m) for an argon discharge, according to the Schottky model. The solid line corresponds to an uniform neutral density. The dashed lines are for nonuniform neutral densities, with $N_0=0.005$ (short-dashed) and $N_0=0.01$ (long-dashed). For all curves, $T_i=T_n=400$ K.

$$n(x) = n_0 \frac{\tan^2\left(K\sqrt{1-(\gamma N_0)^2}\right) - \tan^2\left(K\sqrt{1-(\gamma N_0)^2}x/L\right)}{\tan^2\left(K\sqrt{1-(\gamma N_0)^2}\right) + \tan^2\left(K\sqrt{1-(\gamma N_0)^2}x/L\right)}, \tag{19}$$

with $K \equiv (n_{\mathrm{nw}}L)(\beta_i\beta_c)^{1/2}/(2u_{\mathrm{B}})$. The familiar result $n(x) = n_0\cos(\pi x/2L)$ is easily recovered since $K=\pi/4$ when $\gamma N_0=0$.

It is interesting to note that this solution depends only of γN_0, which can be written as a pressure ratio:

$$\gamma N_0 = \frac{n_0T_e + n_0T_i}{n_{\mathrm{nw}}T_n} \approx \frac{n_0T_e}{n_{\mathrm{nw}}T_n} \equiv \frac{p_{e0}}{p}, \tag{20}$$

where $p_{e0} \equiv n_0T_e$ and $p = n_{\mathrm{nw}}T_n$ are, respectively, the electron pressure at the discharge center and the total pressure. For all practical cases, the ionic pressure $p_i \ll p_e$ since $T_i \ll T_e$. The neutral density at the center of the discharge is obtained from Eq. (14): $n_{n0}/n_{\mathrm{nw}} \approx 1 - p_{e0}/p$. Since $T_n \ll T_e$, a significant neutral depletion at the center of the discharge can appear even for relatively small values of the ionization rate (see the numerical results below).

Equation (17) can be inverted to obtain the electron temperature T_e as a function of the similarity parameter pL ($p/n_{\mathrm{nw}} = k_{\mathrm{B}}T_n/0.133$) for various charged-densities at the center, and is reported in Fig. 1. As expected, the lower the pressure, the higher the electron temperature to maintain the plasma, and we note in addition that taking the dynamics of neutral into account, induces a significant raise in T_e even for rather low ionization rate ($n_0/n_{\mathrm{nw}}=0.005$ and $n_0/n_{\mathrm{nw}}=0.01$ in Fig. 1). Note that as a consequence of (17), the curve is limited to values of T_e and N_0 such that $\gamma N_0 < 1$, a rather strict condition on N_0 since, in all practical cases, $\gamma \gg 1$. In addition, as shown in Fig. 1 for $N_0=0.01$, T_e becomes bivalued for too low pressures: this behavior is consistent with the fact that the model is relevant only for rather high value of pL. These boundaries depend on N_0.

The increase of T_e with N_0 is related to the density profiles reported on Fig. 2 and are obtained from Eqs. (19) and (14). Consistent with the assumption of a high-pressure regime, we choose a rather large value of the similarity parameter: $pL=15$ mTorr m. For all numerical illustrations, we fix

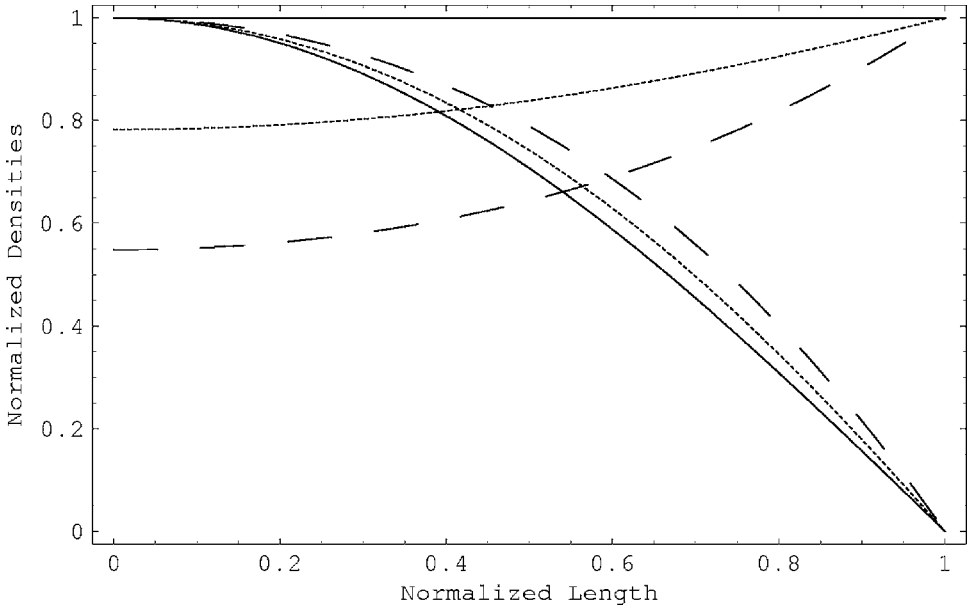

FIG. 2. Charged-particle densities N/N_0 and neutral densities N_n for an argon discharge, as a function of the normalized length x/L, according to the Schottky model. The solid lines correspond to an uniform neutral density. The dashed lines are for non uniform neutral densities, with $N_0=0.005$ (short-dashed) and $N_0=0.01$ (long-dashed). For all curves, $T_i=T_n=400$ K, $pL=15$ mTorr m.

T_n to 400 K. For this particular value of pL, we used (17) to obtain the electron temperatures for some values of N_0 (or for the ionization rate at the center: α_0). We find $T_e=1.43$ eV for uniform neutral densities, $T_e=1.46$ eV for $N_0=0.005$ ($\alpha_0=0.63\%$), and $T_e=1.52$ eV for $N_0=0.01$ ($\alpha_0=1.79\%$). The densities profiles can be understood from the pressure balance equation (14) that we write in the form

$$p = p_n + (p_e + p_i) \approx p_n + p_e,$$

where p_n is the neutral pressure. As a consequence of the depletion effect, the neutral pressure (or the neutral density) increases from the center to the border of the discharge, and the electron pressure (or the electron density) must decrease accordingly. As explained above, we note that for $\alpha_0 \approx 1\%$, the neutral pressure is significantly reduced by a factor of almost 2 at the center of the discharge.

The electrostatic potential profiles are also reported in Fig. 3. As a result of depletion, the potential tend to be uniform across most of the discharge volume, and sharply drop to $-\infty$ at the wall [a consequence of the boundary condition $N(L/\lambda_i)=0$].

III. THE GODYAK MODEL WITH NEUTRAL DYNAMICS

In this section, we solve exactly the Godyak model with neutral dynamics. This model is relevant in the intermediate pressure range. As a by-product of our calculation, we obtain a new explicit formula for the charged-particle density profile in the uniform neutral pressure case.

It is well known (see, for example, Ref. 7) from experimental data, that the constant mobility assumption $v_i \propto E/p$ (where E is the electric field) is only convenient for high

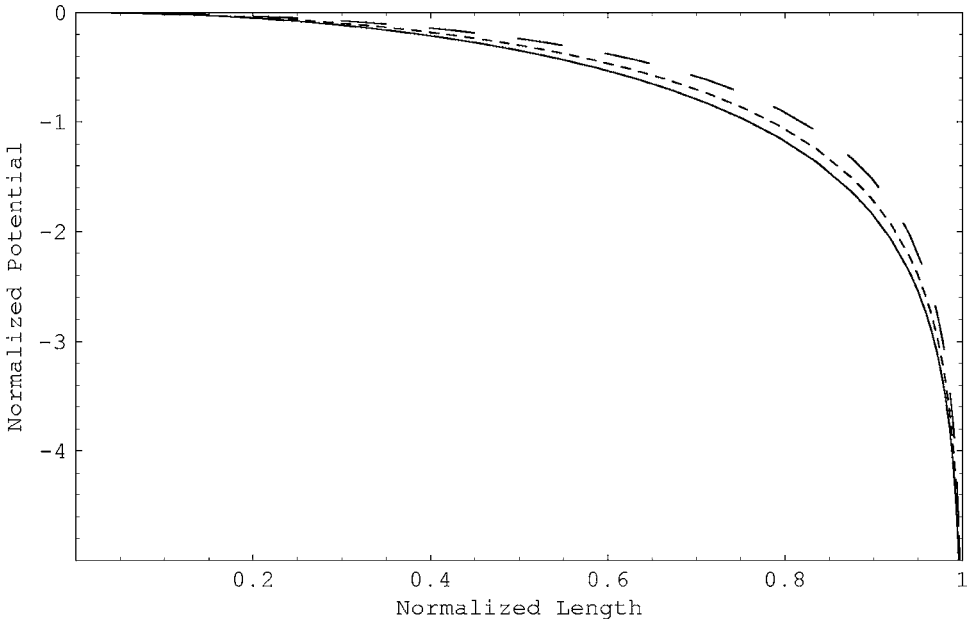

FIG. 3. Electrostatic potential as a function of the normalized length x/L, according to the Schottky model. The solid line corresponds to an uniform neutral density. The dashed lines are for nonuniform neutral densities, with $N_0=0.005$ (short-dashed) and $N_0=0.01$ (long-dashed). For all curves, $T_i=T_n=400$ K, $pL=15$ mTorr m.

pressures p, but breaks down in the intermediate- and low-pressure regimes where $v_i \propto (E/p)^{1/2}$. As long as the ion mobility μ_i is defined by the usual relation $v_i \equiv \mu_i E$, it implies that the ion mobility scales as $\mu_i \sim v_i^{-1}$, the so-called variable mobility assumption. Within this model, ion equilibrium is achieved by the balance between the electric force $qE(x)$ and the nonlinear frictional force $M\sigma_i n_n(x) v_i(x)^2$. Equivalently, the constant parameter $\beta_c \equiv \sigma_i v_{\mathrm{th},i}$ defined for the Schottky model in the preceding section, turns to the nonconstant value $\beta_c(x) \equiv \sigma_i v_i(x)$ in the present Godyak model. A derivation of the ion-neutral collision term in a general form and its reduction to the forms in the Schottky and Godyak models is included in Ref. 8.

In reduced units, the model can be written in the following form:

$$(NV)' = +N_n N, \tag{21}$$

$$(N_n V_n)' = -N_n N, \tag{22}$$

$$N' = -\delta N_n N V^2, \tag{23}$$

$$\gamma^{-1} N_n' = +\delta N_n N V^2, \tag{24}$$

$$\phi = -\ln(N/N_0) \tag{25}$$

with $\delta \equiv \sigma_i u_B / \beta_i$. For uniform neutral densities, this model reduces to the variable mobility model introduced by Godyak in Ref. 3.

Since Eq. (14) still holds, (21) and (23) can be written as

$$\Gamma' = (1 - \gamma N) N, \tag{26}$$

$$N N' = -\delta (1 - \gamma N) \Gamma^2. \tag{27}$$

The neutral density N_n can be eliminated from these equations and using again the boundary conditions, we obtain [compare with Eq. (13)]

$$(N/N_0)^3 + (\Gamma/\Gamma_w)^3 = 1, \tag{28}$$

with $N_0^3 = \delta \Gamma_w^3$. We then use (28) to eliminate Γ from (27):

$$\delta^{1/3} dX = -\frac{N}{1 - \gamma N} \frac{dN}{(N_0^3 - N^3)^{2/3}} = -\sum_{k=0}^{\infty} \gamma^k \frac{N^{k+1}}{(N_0^3 - N^3)^{2/3}} dN, \tag{29}$$

where the use of the series is justified from the inequality $\gamma N < 1$ since $N_n = 1 - \gamma N > 0$ as a density. This equation can be directly integrated between $X = x/\lambda_i$ and the boundary L/λ_i:

$$\frac{3\delta^{1/3}(L - x)}{\lambda_i} = \sum_{k=0}^{\infty} (\gamma N_0)^k \mathrm{B}_{M^3}\left(\frac{k+2}{3}, \frac{1}{3}\right), \tag{30}$$

where $M \equiv N/N_0 = n/n_0$ with $B_x(p,q)$, the incomplete beta function defined by $B_x(p,q) \equiv \int_0^x t^{p-1}(1-t)^{q-1} dt$ (see Ref. 9). Once again, the discharge length L and the parameter γN_0 are not free parameters but are linked by the relation

$$n_{\mathrm{nw}} L = \frac{1}{3}\left(\frac{u_B^2}{\sigma_i \beta_i^2}\right)^{1/3} \sum_{k=0}^{\infty} (\gamma N_0)^k \mathrm{B}\left(\frac{k+2}{3}, \frac{1}{3}\right) \tag{31}$$

obtained for $x = 0$, where $M = 1$ and $B(p,q)$ is the (complete) beta function defined by $B(p,q) \equiv \int_0^1 t^{p-1}(1-t)^{q-1} dt$ (also see Ref. 9).

Finally, the density $M(x) = n(x)/n_0$ is given in closed form in terms of beta functions by the inverse relation

$$\frac{x}{L} = 1 - \frac{1}{3 n_{nw} L}\left(\frac{u_B^2}{\sigma_i \beta_i^2}\right)^{1/3} \sum_{k=0}^{\infty} (\gamma N_0)^k \mathrm{B}_{M^3}\left(\frac{k+2}{3}, \frac{1}{3}\right). \tag{32}$$

It is interesting to show that this expression can be used to recover quite efficiently the tricky calculations performed in Ref. 3 or in Ref. 6 for the uniform neutral case. In that case, it is sufficient to retain only the first term in the series ($k = 0$) to obtain

$$n_{\mathrm{nw}} L = \frac{1}{3}\left(\frac{u_B^2}{\sigma_i \beta_i^2}\right)^{1/3} B\left(\frac{2}{3}, \frac{1}{3}\right), \tag{33}$$

$$n(x) = n_0 \left[K\left(\frac{2}{3}, \frac{1}{3}, 1 - \frac{x}{L}\right)\right]^{1/3}, \tag{34}$$

where $K(a,b,s)$ is the solution for z in $s = B_z(a,b)/B(a,b)$ (the K-function can be obtained from the MATHEMATICA software by a single command). Expressions (33) and (34) are new, but are equivalent forms of those given in Ref. 3 or in Ref. 6.

Equations (31) is used and reported in Fig. 4 to obtain the electron temperature T_e as a function of pL. The charged-particle and neutral densities are obtained from Eqs. (32) and (14) and are plotted in Fig. 5. Using the same procedure as for the Schottky model, we fix pL to the intermediate value $pL = 3$ mTorr m, and obtain the electron temperatures $T_e = 1.96$ eV, $T_e = 2.06$ eV and $T_e = 2.31$ eV, respectively, for the uniform pressure case, for $N_0 = 0.005$ ($\alpha_0 = 0.71\%$) and for $N_0 = 0.01$ ($\alpha_0 = 3.02\%$). Last, using $\phi = -\ln(N/N_0)$, the potential profiles are reported in Fig. 6. The behaviors observed for the Godyak model are qualitatively the same than for the Schottky model. We note that, as a consequence of a more efficient friction force at high velocities, the densities and potential profiles are flatter.

IV. THE TONKS-LANGMUIR MODEL WITH NEUTRAL DYNAMICS

In the very low-pressure limit, the ion mean free path becomes larger than the discharge length. In this limit, the validity of a fluid approach is dubious, and a kinetic model must be used. The kinetic model, first introduced by Tonks and Langmuir in Ref. 1, was later analytically solved for a one-dimensional plane geometry by Harrison and Thompson in Ref. 10 and by Self and Ewald in Ref. 11. Kino and Shaw, as given in Ref. 12, compared this model to a simplified fluid-like approach. Caruso and Cavaliere investigated the Tonks-Langmuir model with neutral depletion, but with some particular assumptions on the velocities of the neutral particles in Ref. 13. In this section, we improve the Caruso and Cavaliere analysis by treating self-consistently the neu-

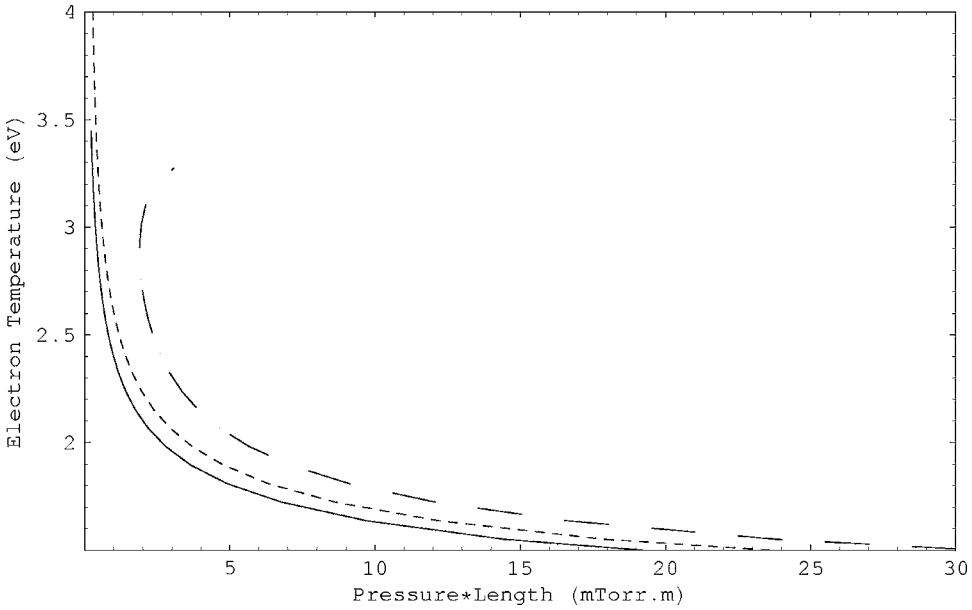

FIG. 4. Electron temperature T_e (in K) as a function of the similarity parameter pL (in mTorr m) for an argon discharge, according to the Godyak model. The solid line corresponds to an uniform neutral density. The dashed lines are for nonuniform neutral densities, with $N_0=0.005$ (short-dashed) and $N_0=0.01$ (long-dashed). For all curves, $T_i=T_n=400$ K.

tral dynamics in the Tonks-Langmuir approach. We get an hybrid model with kinetic equations for ions, whereas electrons and neutrals are still described by fluid equations.

The equations of continuity (1) and (4) are still correct, but the momentum equation for neutrals is written in the following form:

$$Mn_n(x)v_n(x)\frac{dv_n(x)}{dx}+k_BT_n\frac{dn_n(x)}{dx}=0, \tag{35}$$

(see Appendix A for details). As before, we assume isothermal neutrals. Integrating this expression with the previous normalizations and $N_{\mathrm{nw}}=1$, we obtain

$$\frac{\Gamma_n^2}{2N_n^2}+\gamma^{-1}\ln N_n=\frac{\Gamma_{\mathrm{nw}}^2}{2}=\gamma^{-1}\ln N_{n0}, \tag{36}$$

where $\Gamma_n\equiv N_nV_n$ and $\Gamma_{\mathrm{nw}}\equiv\Gamma_n(L/\lambda_i)$ are, respectively, the neutral flux at the position X and at the wall. From (36), the neutral density at the center of the discharge, i.e., $N_{n0}\equiv n_{n0}/n_{\mathrm{nw}}$, is such that

$$N_{n0}=e^{\gamma\Gamma_{\mathrm{nw}}^2/2}>1. \tag{37}$$

Hence, we conclude that the effect of depletion is reversed in this low-pressure limit: the neutral density presents a maximum at the center of the discharge. Indeed, when the drag on neutrals due to collisions with ions is negligible, the balance energy cannot reduce to a pressure balance as in the high-pressure limit, but neutral dynamics result from a balance between inertial and pressure terms.

We turn now to the ion dynamics. Within the Tonks-Langmuir theory, ions are falling freely through the plasma from their points of origin with a negligible initial velocity. Hence, ions generated at a rate $g(z)dz$ in the volume element dz at z attain at $x\geqslant z$ a velocity

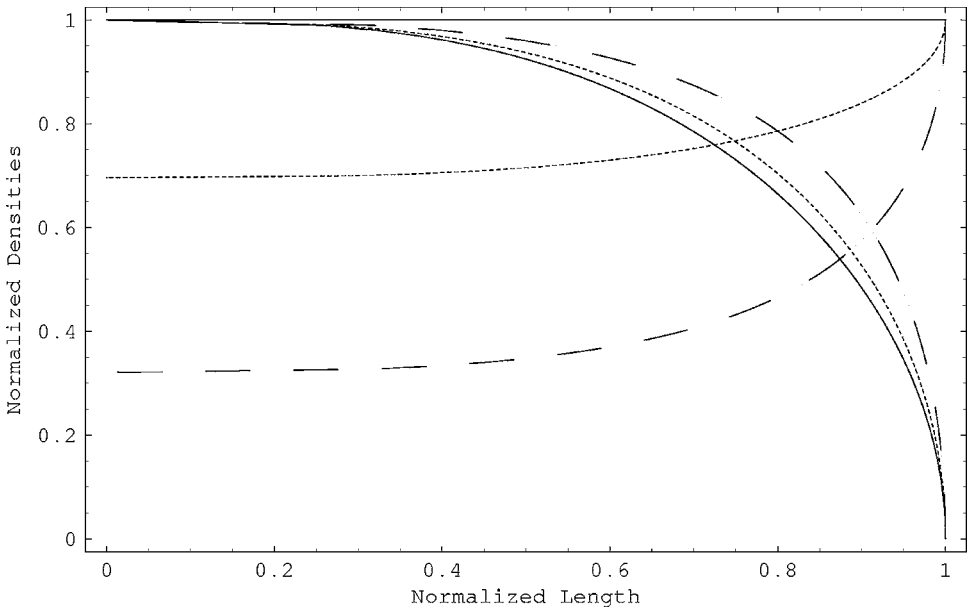

FIG. 5. Charged-particle densities N/N_0 and neutral densities N_n for an argon discharge, as a function of the normalized length x/L, according to the Godiak model. The solid lines correspond to an uniform neutral density. The dashed lines are for nonuniform neutral densities, with $N_0=0.005$ (short-dashed) and $N_0=0.01$ (long-dashed). For all curves, $T_i=T_n=400$ K, $pL=3$ mTorr m.

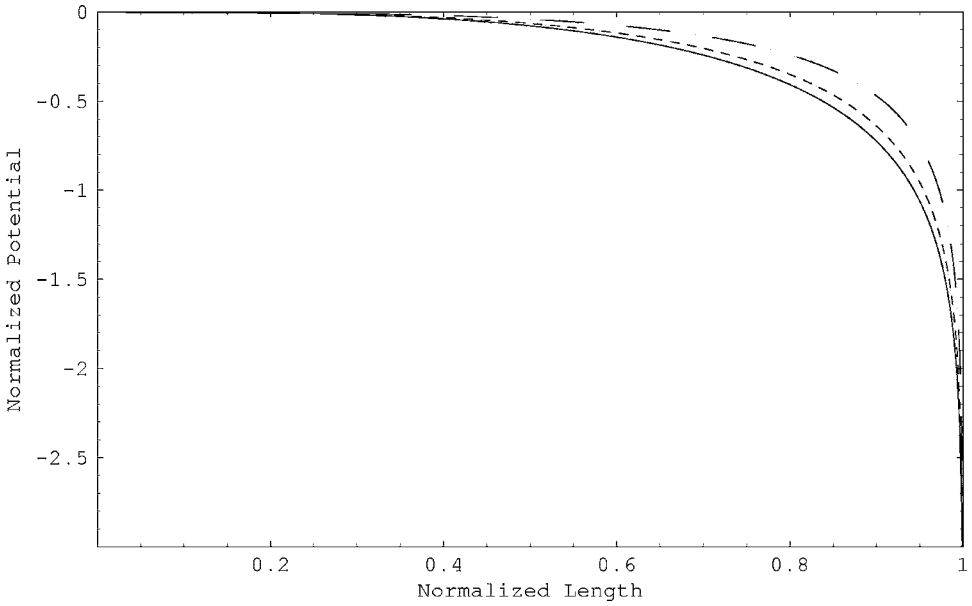

FIG. 6. Electrostatic potential as a function of the normalized length x/L, according to the Godyak model. The solid line corresponds to an uniform neutral density. The dashed lines are for nonuniform neutral densities, with $N_0=0.005$ (short-dashed) and $N_0=0.01$ (long-dashed). For all curves, $T_i=T_n=400$ K, $pL=3$ mTorr m.

$$v(x,z)=\left\{\frac{2e}{M}[\varphi(z)-\varphi(x)]\right\}^{1/2}.$$

The ion velocity distribution is then $f(v)dv=g(z)dz/v(x,z)$ and the resulting ion density may be written

$$n_i(x)=\left(\frac{M}{2e}\right)^{1/2}\int_0^x\frac{g(z)dz}{[\varphi(z)-\varphi(x)]^{1/2}}. \tag{38}$$

Electrons are always considered in thermal equilibrium, and their number density is given by $n_e(x)=n_0e^{e\varphi(x)/k_BT_e}$. Again, we assume quasineutrality: $n_i(x)=n_e(x)$. Using the same normalizations as above, the relevant normalized equations are

$$\Gamma_n'=-N_nN, \tag{39}$$

$$N(X)=2^{-1/2}\int_0^X\frac{N_n(Z)N(Z)dZ}{[\phi(X)-\phi(Z)]^{1/2}}, \tag{40}$$

$$N=N_0e^{-\phi}, \tag{41}$$

$$\Gamma_{\rm nw}^2=\frac{\Gamma_n^2}{N_n^2}+\gamma^{-1}\ln N_n^2. \tag{42}$$

These equations must be solved with the boundary conditions

$$\Gamma_n(0)=0,\quad \phi(0)=0,\quad N_n(L/\lambda_i)=1.$$

Combining Eqs. (40) and (41), and making the change of variables $X\rightarrow\phi(X)$, we obtain

$$2^{1/2}N_0e^{-\phi}=\int_0^\phi\frac{N_n(\psi)N(\psi)}{(\phi-\psi)^{1/2}}\frac{dZ}{d\psi}d\psi. \tag{43}$$

This equation has the form of an Abel integral, which can be inverted by Laplace transform. We find:

$$N_n(\phi)N(\phi)\frac{dX}{d\phi}=\frac{2^{1/2}N_0}{\pi}\left[\frac{1}{\phi^{1/2}}-\int_0^\phi\frac{e^{-\psi}}{(\phi-\psi)^{1/2}}d\psi\right]$$
$$\equiv\frac{2^{1/2}N_0}{\pi}C(\phi). \tag{44}$$

The integral in $C(\phi)$ can be performed in terms of the error function $\mathrm{erfi}(x)\equiv 2\pi^{-1/2}\int_0^x e^{u^2}du$,[9] with the result:

$$C(\phi)=\frac{1}{\phi^{1/2}}-\pi^{1/2}e^{-\phi}\,\mathrm{erfi}(\phi^{1/2}). \tag{45}$$

One notices from (44) that the electric field $d\phi/dX$ is infinitely large at some value of the potential ϕ_w, which solves the equation $C(\phi_w)=0$, or

$$e^{\phi_w}=(\pi\phi_w)^{1/2}\,\mathrm{erfi}(\phi_w^{1/2}). \tag{46}$$

This particular value of the potential (numerically, $\phi_w=0.854$) is the extreme limit of validity of the Tonks-Langmuir boundary (that we identify with the position of the wall), and is the same as for the case of uniform neutral pressure, which is presented in Ref. 10.

Equation (44) can be integrated in the form

$$\frac{x}{L}=\frac{2^{1/2}}{\pi}\frac{u_B}{\beta_i(n_{\rm nw}L)}\int_0^\phi\frac{C(\psi)e^{+\psi}}{N_n(\psi)}d\psi. \tag{47}$$

Since $C(\phi)$ is known, if the neutral density is obtained as a function of the potential ϕ, the problem is solved. To obtain $N_n(\phi)$, we first note that Eq. (39) can be recast in the form

$$\frac{d\Gamma_n}{d\phi}=-N_nN\frac{dX}{d\phi}.$$

Hence, again using Eq. (44) and the boundary condition $\Gamma_n(0)=0$, we obtain

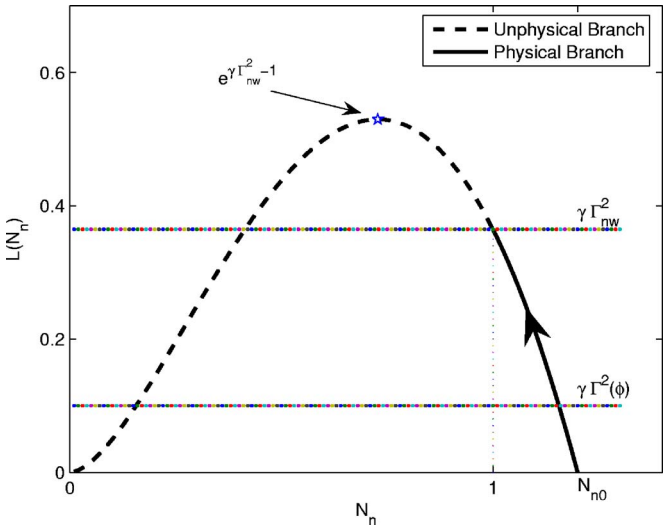

FIG. 7. The momentum equations for neutrals in the form of Eq. (50) (see text).

$$\Gamma_n(\phi) = -\frac{2^{1/2}N_0}{\pi}\int_0^{\phi} C(\psi)d\psi$$

$$= -\left(\frac{2}{\pi}\right)^{1/2} N_0 e^{-\phi}\,\mathrm{erfi}(\phi^{1/2}). \tag{48}$$

The neutral flux at the wall can be obtained from this expression and equation (46): $\Gamma_{nw}=-2^{1/2}N_0/(\pi\phi_w^{1/2})$, and hence, the density of neutrals at the center is given explicitly by

$$N_{n0} = e^{\gamma N_0^2/(\pi^2\phi_w)} \approx e^{0.119\gamma N_0^2}. \tag{49}$$

Let us recast Eq. (42) in the following form:

$$\mathcal{L}[N_n] \equiv \ln(N_{n0}^2)N_n^2 - N_n^2\ln(N_n^2) = \gamma\Gamma_n^2(\phi), \tag{50}$$

where we used the relation $\gamma\Gamma_{nw}^2=\ln(N_{n0}^2)$. We report $\mathcal{L}[N_n]$ as a function of N_n in Fig. 7. It is clearly shown that Eq. (50) has two solutions for $N_n(\phi)$ when $\gamma\Gamma_n^2(\phi)$ is lower than the critical value $e^{\gamma\Gamma_{nw}^2-1}$, and none in the other case. In fact, since $e^{\gamma\Gamma_{nw}^2-1} \geqslant \gamma\Gamma_{nw}^2$, this critical value is never attained. Since Γ_n is a monotonically decreasing function from $\phi=0$ to $\phi=\phi_w$, while N_n varies from N_{n0} to 1, the relevant branch of $\mathcal{L}[N_n]$ is (a part of) the decreasing one (see Fig. 7). Straightforward algebra shows that at the critical value $\gamma\Gamma_n^2=N_n^2$, or $V_n=\gamma^{-1/2}$. In other words, the neutral velocity would reach its thermal velocity $v_n=(k_BT_n/M)^{1/2}$ at the critical point. Nevertheless, as mentioned above, the critical point is not accessible, and we conclude, as expected, that the neutral velocity is quite small, but not uniform, in all the volume of the discharge.

From these remarks and Eq. (50), the neutral density as a function of the electrostatic potential can be obtained in closed form from the expression

$$N_n(\phi) = \frac{\gamma^{1/2}\Gamma_n(\phi)}{[T_0(\gamma\Gamma_n^2(\phi)/N_{n0}^2)]^{1/2}}, \tag{51}$$

where $T_0(x)$ is the principal branch of tree function defined by the relation $T(x)e^{-T(x)}=x$. This tree function is related to the Lambert W function (see Appendix B for details). The electron temperature is determined from Eq. (47) for $x=L$. Hence:

$$n_{nw}L = \frac{2^{1/2}}{\pi}\frac{u_B}{\beta_i}\int_0^{\phi_w}\frac{C(\psi)e^{+\psi}}{N_n(\psi)}d\psi. \tag{52}$$

We use this equation together with (51) to obtain the electron temperature T_e as a function of the similarity parameter pL, for various densities at the center (N_0). Since this model is valid for very low pressures, we restrict the domain of pL to $pL<1$ mTorr m (cf. Fig. 8). We see that, upon increasing N_0, results in a lower effective electron temperature, a consequence of the reversed depletion effect. Note in addition that in this low-pressure regime, the coupling between neutrals and ions is small, and consequently larger values of N_0 (compared with the other pressure regimes) must be used, in order

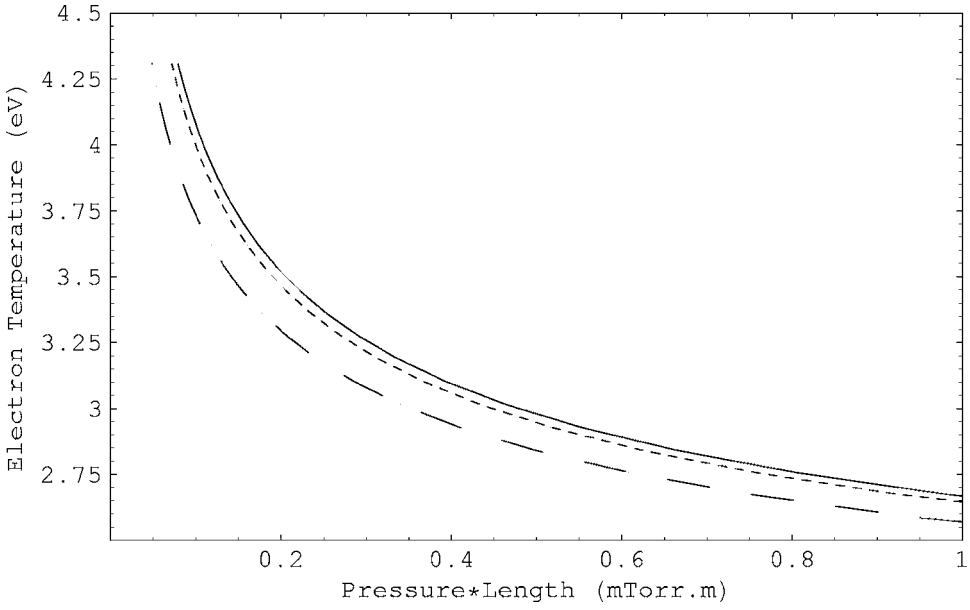

FIG. 8. Electron temperature T_e (in K) as a function of the similarity parameter pL (in mTorr m) for an argon discharge, according to the Tonks-Langmuir model. The solid line corresponds to an uniform neutral density. The dashed lines are for nonuniform neutral densities, with $N_0=0.1$ (short-dashed) and $N_0=0.2$ (long-dashed). For all curves, $T_i=T_n=400$ K.

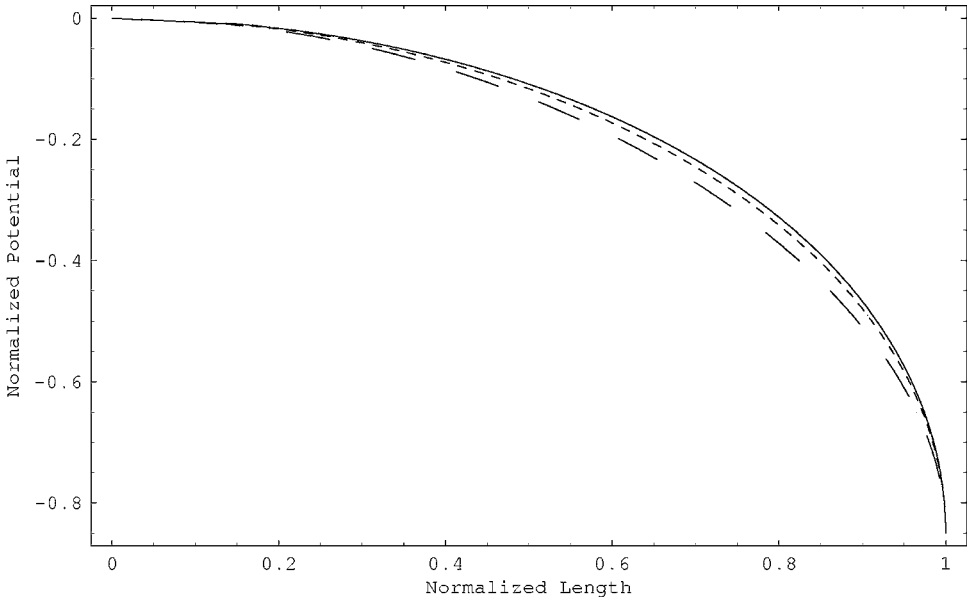

FIG. 9. Electrostatic potential as a function of the normalized length x/L, according to the Tonks-Langmuir model. The solid line corresponds to an uniform neutral density. The dashed lines are for nonuniform neutral densities, with $N_0=0.1$ (short-dashed) and $N_0=0.2$ (long-dashed). For all curves, $T_i=T_n=400$ K, $pL=0.2$ mTorr m.

to see any quantitative effect relative to the uniform neutral density case ($N_0=0.1$ and $N_0=0.2$ in Fig. 8).

The electrostatic potential as a function of the normalized length x/L is obtained from Eq. (47) and reported in Fig. 9. The curves are plotted for $pL=0.2$ mTorr m, and the corresponding electron temperatures, obtained from (52), are found to be $T_e=3.52$ eV, $T_e=3.47$ eV, and $T_e=3.29$ eV, respectively, for the uniform pressure cases $N_0=0.1$ and $N_0=0.2$. Again, and for the same reasons, the greater the density is at the center, the lower is the potential. Note that contrary to the precedings cases, the potential at the wall is finite, and so is the density: $N_w=N_0e^{-\phi_w}$. Consequently, the boundary condition used at higher pressures, i.e., $N(L/\lambda_i)=0$, is not relevant for this case and was not used. Last, once the electrostatic potential known, the ion and neutral densities are obtained from the relation $N=N_0e^{-\phi}$ and from Eq. (51), with the behavior mentioned above (see Fig. 10).

V. DISCUSSION AND CONCLUSIONS

In this section, we compare the three models detailed in the previous sections, and we underline the limits of our work.

A key point of our analysis has been to show that particle and energy balance are both necessary to determine the electron temperature when the dynamics of neutrals is included in the models. We have reported in Fig. 11 the electron temperature T_e as a function of the similarity parameter pL, for the three models when $N_0=0.005$. As an indicator, we also plot the usual boundary between Schottky and Godyak models given by $\lambda T_e/LT_n \approx 1$ for the undepleted case. As can be seen in Fig. 11, this boundary and the crossing point of the two curves are close. It will be of interest to compare these results with experimental measurements. It is instructive to compare the three equations (17), (31), and (52),

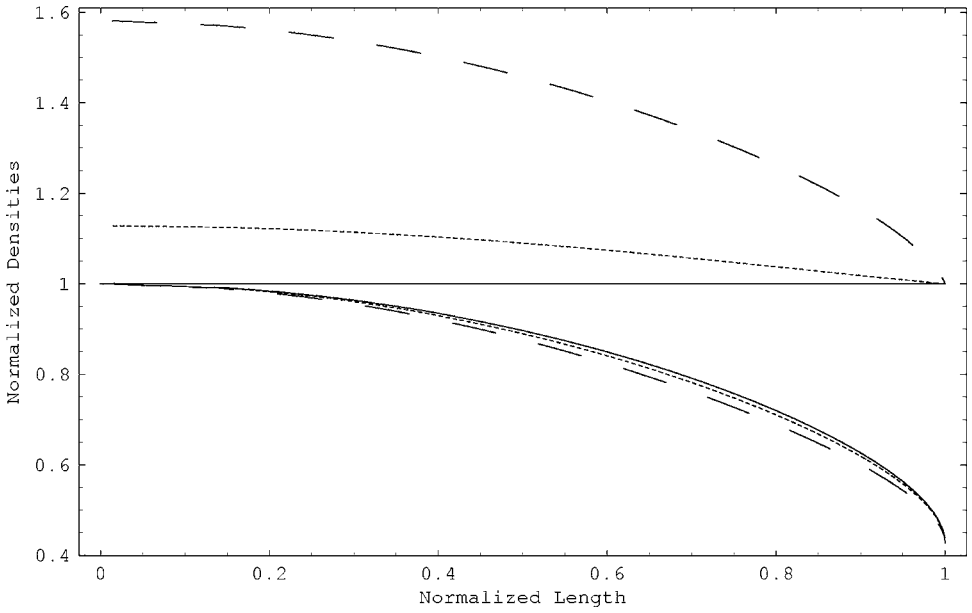

FIG. 10. Charged-particle densities N/N_0 and neutral densities N_n for an argon discharge, as a function of the normalized length x/L, according to the Tonks-Langmuir model. The solid line correspond to an uniform neutral density. The dashed lines are for nonuniform neutral densities, with $N_0=0.1$ (short-dashed) and $N_0=0.2$ (long-dashed). For all curves, $T_i=T_n=400$ K, $pL=0.2$ mTorr m.

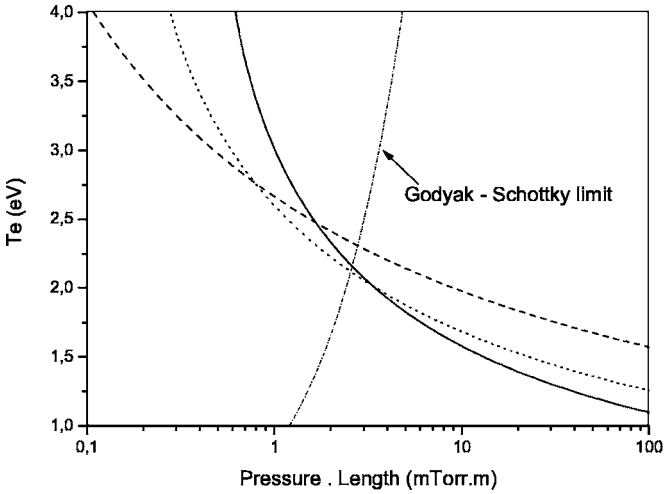

FIG. 11. Electron temperature T_e (in K) as a function of the similarity parameter pL (in mTorr m) for an argon discharge, according to the Schottky model (solid line), to the Godyak model (short-dashed line), and to the Tonks-Langmuir model (long-dashed line). The dot-dashed line is the usual boundary beween the Schottky and Godyak models $\lambda T_e/LT_n \approx 1$ for the undepleted case. For all curves, $T_i=T_n=400$ K, and $N_0=0.005$.

which fixed the electron temperature for each model. These equations can be recast in the compact form:

$$L^2 \sim \lambda_i \lambda_c f_S(\gamma N_0), \tag{53}$$

$$L^3 \sim \lambda \lambda_i^2 f_G(\gamma N_0), \tag{54}$$

$$L \sim \lambda_i f_{TL}(\gamma N_0^2). \tag{55}$$

In these expressions, $\lambda_i \equiv u_B/(\beta_i n_{nw})$ is the ionization length, $\lambda_c \equiv u_B/(\beta_c n_{nw})$ is the collisional length, and $\lambda \equiv (n_{nw}\sigma_i)^{-1}$ is the ion mean free path. All these lengths are defined at the wall. The dependence on the charged-particle density at the center, which is characteristic of the neutral dynamics, is contained for the three models in a specific function which depends only on the pressure ratio γN_0 for the two high-pressure models, and on γN_0^2 for the low-pressure model. The dependence on the various lengths is also characteristic of the underlying physical processes. The Schottky form, $L^2 \sim \lambda_i \lambda_c$, is diffusive in its origin. Indeed, if N collisions are necessary to reach the wall, then, for a diffusive process: $L^2=N\lambda_c^2$, while $N\lambda_c=\lambda_i$ is the *ad hoc* criteria necessary for the existence of the discharge (in other words, one ionization at least must occur in the discharge before the electron is lost at the wall). Since there is no collision in the Tonks-Langmuir model, the only length is the ionization length and the process is ballistic as it must. In accordance with the assumptions underlying Godyak model, transport coefficients are not uniform, and the resulting scaling is related to a nonlinear diffusive process.

It was pointed out in Ref. 4 that the total number of neutrals can be interpreted as a generalized similarity parameter for the Schottky and Godyak models. In fact, the link between electron temperature and the total number of neutrals is universal and valid for the three models. For the Tonks-Langmuir case, using the relation $\Gamma_n=-\Gamma$ and Eq. (39) we have

$$N_T \equiv \int_0^{L/\lambda_i} N_n dX = \int_0^{\phi_w} \frac{1}{N}\frac{d\Gamma}{d\phi} d\phi.$$

Since $d\Gamma/d\phi \propto C(\phi)$ from Eq. (48), we find after integration,

$$N_T = \frac{1}{2^{1/2}\pi}\frac{e^{+\phi_w}}{\phi_w^{1/2}} \approx 0.572 \quad \text{(Tonks-Langmuir model)}, \tag{56}$$

where we use again Eq. (46). Let us derive for completeness the corresponding equations for the collisional cases. From the equation of continuity for ions, we have

$$N_T = \int_0^{\Gamma_w} \frac{d\Gamma}{N} = \frac{\Gamma_w}{N_0}\int_0^1 \frac{d\Gamma/\Gamma_w}{N/N_0}.$$

Since the curves in the plane (Γ, N) are known, i.e., a circle for the Schottky model [Eq. (13)], or a Fermat curve for the Godyak model [Eq. (28)], we immediately obtain the relations

$$\frac{2}{\pi}N_T = \left(\frac{\lambda_c}{\lambda_i}\right)^{1/2} \quad \text{(Schottky model)}, \tag{57}$$

$$\frac{3}{B(2/3,1/3)}N_T = \left(\frac{\lambda}{\lambda_i}\right)^{1/3} \quad \text{(Godyak model)}, \tag{58}$$

where we used $\tau=N_0^2/\Gamma_w^2=\lambda_i/\lambda_c$ (Schottky) and $\delta=N_0^3/\Gamma_w^3=\lambda_i/\lambda$ (Godyak). These equations are the same as Eqs. (6) and (12) of Ref. 4 [since $B(2/3,1/3)=2\pi/\sqrt{3}$]. When neutrals are not depleted ($N_T=L/\lambda_i$), we recover Eqs. (18) and (33) of the present paper. Equations (56)–(58), are universal relations between the total number of neutrals and the electron temperature.

In accordance with some earlier studies (see, for example, Ref. 4), a neutral depletion occurs at the center of the discharge when the neutral dynamics is governed by collisions with ions. However, in the collisionless limit, we have shown that the discharge exhibits a maximum at the center of the discharge. The neutral depletion (or the opposite) can be easily quantified for the three models studied. The magnitude of the neutral density at the center of the discharge is obtained from (14) for mobility-limited models, and from (49) for inertia-limited models:

$$N_{n0} = 1 - \gamma N_0 \quad \text{(mobility-limited models)},$$

$$N_{n0} = e^{0.119\gamma N_0^2} \quad \text{(inertia-limited models)}.$$

These very simple formulas show that the neutral density at the center of the discharge, depends only on the temperature ratio $\gamma \approx T_e/T_n$ and on the ionization rate at the center $\alpha_0 \approx n_0/n_{nw}$. For most discharges, $T_e/T_n \approx 100$, and we note that an ionization rate as small as 0.5%, is associated with a depletion effect of 50% for mobility-limited models, while the corresponding opposite effect for inertia-limited model is limited to 0.3%. Hence, we predict that reversed depletion could only be observed with an intense ionization in the discharge.

These theories of neutral gas transport in plasma discharges can be extended in various directions. First, the

quasineutrality assumption can be easily removed, and the densities or potential profiles can be obtained at the expense of some numerical work. The charged-particle density at the center, i.e., N_0, is fixed by the power deposited in the discharge. Since the power is an experimental input parameter, it can be of interest to reformulate these theories in term of this parameter. A limitation of our work is the isothermal hypothesis for neutrals. Some detailed numerical works (see Refs. 14 and 15) have shown that the electron temperature and ion temperature varies only slightly across the column, except very close to the wall. Indeed, recent experimental measurements, as given in Ref. 5, have reported strong neutral depletion at the center of the discharge, together with almost uniform electron temperature. However, neutral-gas heating has been observed in recent experiments, as Ref. 16, and have to be taken into account. We believe that this will be a significant effect. In an hydrodynamic approach, it implies to build a three-fluid model retaining the third first moments of the Boltzmann equation. Work along this line is currently on progress.

APPENDIX A: THE NEUTRAL EQUATION OF MOTION IN THE COLLISIONLESS CASE

In this appendix, we derive the momentum equation for neutrals used in the Tonks-Langmuir model [Eq. (35)].

The evolution of the neutral and ion distribution functions, f_n and f_i, respectively, in the presence of ionizing collisions only is determined by the Boltzmann equations

$$\frac{\partial f_n}{\partial t} + \frac{\partial (v f_n)}{\partial x} = -\beta_i n_e f_n,$$

and

$$\frac{\partial f_i}{\partial t} + \frac{\partial (v f_i)}{\partial x} + \frac{\partial}{\partial v}\left(\frac{eE}{M} f_i\right) = \beta_i n_e f_n.$$

The term on the right-hand side of the equations expresses ionization. Integrating the equations over the velocity we obtain the continuity equations [reduced for the ions in a steady state to Eq. (1)]. Multiplying the equations by Mv and integrating over v, we obtain the momentum equations

$$M\frac{\partial (n_n v_n)}{\partial t} + \frac{\partial (M n_n v_n^2 + p_n)}{\partial x} = -M\beta_i n_e n_n v_n, \tag{A1}$$

and

$$M\frac{\partial (n_i v_i)}{\partial t} + \frac{\partial (M n_i v_i^2 + p_i)}{\partial x} - eEn_i = M\beta_i n_e n_n v_n.$$

Note that if $v_i \gg v_n$ one can easily show, using the continuity equation, that the drag term on the right-hand side of the ion momentum equation is negligible relative to the inertia term. For the neutrals, however, this term cannot be neglected. Employing the neutral continuity equation, and assuming a steady state and a uniform neutral temperature, Eq. (A1) takes the form given as Eq. (35).

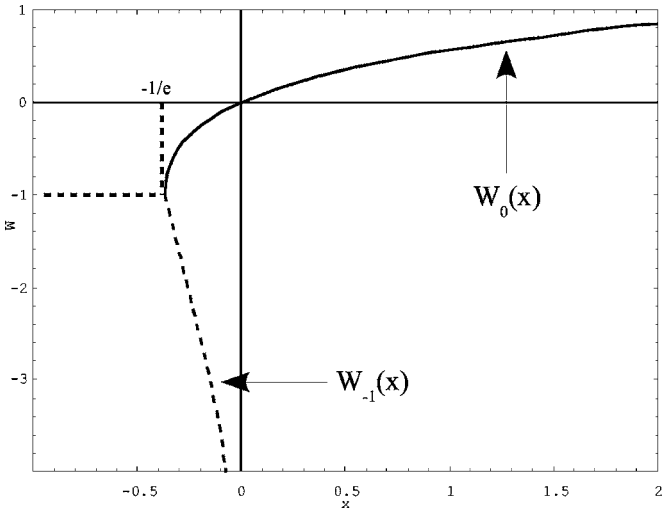

FIG. 12. The two branches of the Lambert function: the principal branch $W_0(x)$ satisfying $W_0(x) \geqslant -1$, and the branch $W_{-1}(x)$ satisfying $W_{-1}(x) \leqslant -1$ (see Appendix B).

APPENDIX B: SOME PROPERTIES OF THE TREE AND LAMBERT FUNCTIONS

The Lambert function W is defined to be the function that solves the equation

$$W(x)\mathrm{e}^{W(x)} = x, \tag{B1}$$

with x real or complex. This function has many applications in physics and applied mathematics, and has been recently implemented in various computer algebra systems such as MAPLE or MATHEMATICA. A nice review is given in Ref. 17. Here, we just give some elementary results on this function in order to understand the derivations performed in Sec. IV.

Taking the logarithm of Eq. (B1) and posing $W \equiv Y^n$ (with n a positive or negative exponent) and $\ln x \equiv c$, we obtain the equation

$$Y^n + n\ln(Y) = c. \tag{B2}$$

In physical terms, this form is reminiscent of a balance energy equation between an entropic term and an interaction term. This is probably the reason this function occurs so often in such various physical situations. The link with Eq. (36) of the present paper is obvious.

Equation (B1) has generally many solutions, being possibly complex, and hence, W is a multivalued function. An important example is the case of x being real. In that case (see Fig. 12), there is no real solution when $x < -\mathrm{e}^{-1}$, two possible real values when $-\mathrm{e}^{-1} \leqslant x < 0$, and one real when $x > 0$. The branch satisfying $W(x) \geqslant -1$ is referred to as the principal branch of the W function and is denoted $W_0(x)$, while the branch satisfying $W(x) \leqslant -1$ is denoted $W_{-1}(x)$.

The tree function T is related to the Lambert function by the relation $T(x) = -W(-x)$, and hence the tree function verifies

$$T(x)\mathrm{e}^{-T(x)} = x. \tag{B3}$$

Its name comes from the fact that its Taylor expansion, i.e., $T(x) = \Sigma_n t_n x^n / n!$, is such that the coefficients t_n are the num-

ber of rooted trees on n labeled points. Since $t_n = n^{n-1}$, the expansion of the tree function is given by

$$T(x) = x + x^2 + \frac{3}{2}x^3 + \frac{8}{3}x^4 + \cdots . \tag{B4}$$

This formula can be used to obtain the first terms of the series expansion of the neutral density as a function of ϕ [Eq. (51)].

[1] L. Tonks and I. Langmuir, Phys. Rev. **34**, 876 (1929).
[2] W. Schottky, Phys. Z. **25**, 635 (1924).
[3] V. Godyak, *Soviet Radiofrequency Discharge Research* (Delphic Associates, Fall Church, VA, 1986), pp. 80–88.
[4] A. Fruchtman, G. Makrinich, P. Chabert, and J.-M. Rax, Phys. Rev. Lett. **95**, 115002 (2005).
[5] S. Yun, K. Taylor, and G. R. Tynan, Phys. Plasmas **7**, 3448 (2000).
[6] M. Lieberman and A. Lichtenberg, *Principles of Plasma Discharges and Materials Processing*, 2nd ed (Wiley, New York, 2005), p. 81.
[7] R. N. Franklin, *Plasma Phenomena in Gas Discharges* (Oxford University Press, 1976), p. 2.
[8] A. Fruchtman, G. Makrinich, and J. Ashkenazy, Plasma Sources Sci. Technol. **14**, 152 (2005).
[9] I. Gradshteyn and I. Ryzhik, *Table of Integrals, Series and Products* (Academic, 1980), p. 950.
[10] E. R. Harrison and W. B. Thompson, Proc. Phys. Soc. London **74**, 145 (1959).
[11] S. Self and H. N. Ewald, Phys. Fluids **9**, 2486 (1966).
[12] G. S. Kino and E. K. Shaw, Phys. Fluids **9**, 587 (1966).
[13] A. Caruso and A. Cavaliere, Br. J. Appl. Phys. **15**, 1021 (1964).
[14] D. B. Ilic, J. Appl. Phys. **44**, 3993 (1973).
[15] H.-B. Valentini, D. Wolff, and E. Glauche, J. Phys. D **28**, 716 (1995).
[16] H. Abada, P. Chabert, J.-P. Booth, J. Robiche, and G. Cartry, J. Appl. Phys. **92**, 4223 (2002).
[17] R. M. Corless, G. H. Gonnet, D. E. G. Hare, D. J. Jeffrey, and D. E. Knuth, Adv. Comput. Math. **5**, 329 (1996).